Electrochemical Measurement of the Solvent Accessibility of Nucleobases Using Electron Transfer between DNA and Metal Complexes

Dean H. Johnston,† Katherine C. Glasgow, and H. Holden Thorp*

Contribution from the Department of Chemistry, University of North Carolina at Chapel Hill, Chapel Hill, North Carolina 27599-3290

Received April 24, 1995[⊗]

Abstract: Oxidizing metal complexes mediate the electrochemical oxidation of guanine nucleotides in polymeric DNA and oligonucleotides. This catalysis results in an enhancement in cyclic voltammograms that yields the rate constant for oxidation of guanine by the metal complex via digital simulation. The rate constant for oxidation of guanine in calf thymus DNA by $Ru(bpy)_3^{3+}$ is 9.0×10^3 M^{-1} s^{-1}, which has been confirmed in separate experiments utilizing pulsed voltammetry and stopped-flow spectrophotometry. The rate constant depends linearly on the driving force with a slope of $^1/_2$, as predicted by Marcus theory. Formation of the double helix precludes direct collision of the metal complex with the guanine residue, which imposes a finite distance of solvent through which the electron must tunnel. This distance is dependent on the presence of the oxidized guanine in a mismatch, which decreases the tunneling distance as assessed from electron-transfer theory. The oxidation rate constants therefore follow the trend G (single strand) > GA > GG > GT > GC. These mismatches are all distinguishable from one another, providing a new basis for probing small changes in the solvent accessibility of guanine that may be useful in DNA sequencing or quantitatively mapping complex nucleic acid structures.

The detection of individual DNA sequences in heterogeneous samples of polymeric DNA provides a basis for identifying genes, DNA profiling, and novel approaches to DNA sequencing.[1−5] These applications may involve recognition events either between two single strands to form a double helix or between a third strand and a duplex to form a triple helix.[6,7] Recent advances in photolithography have led to "DNA chips" where many DNA sequences are assembled on individual loci on a surface.[8−10] Using these novel surfaces, multiple sequences can be assayed in a single experiment using an analytical response that indicates hybridization of the surface-bound oligomer to a sequence in the heterogeneous sample. These analytical methods generally involve laser-induced fluorescence arising from a covalently attached label on the target DNA strand, which is not sensitive to single-base mismatches in the surface-bound duplex, although mismatches can be detected in enzymatic or chemical cleavage studies.[11−13] These mismatches will be unavoidable when assaying for multiple sequences with different melting temperatures in the same experiment.

Two potential approaches to electron-transfer-based hybridization assays have been reported. One approach involves immobilization of single-stranded DNA on an electrode surface with a cationic metal complex in the bulk solution.[14−16] The concentration of the metal complex at the electrode surface increases when hybridization of the immobilized DNA to the target strand occurs because the metal complex has a much higher affinity for double-stranded DNA. As a result, enhanced reduction current or electrogenerated chemiluminescence signals hybridization. The unique feature of duplex DNA that is detected in this approach is a higher affinity for bound cations, and combination of this molecular signal with the high sensitivity afforded by surface immobilization[14,17] and electrogenerated chemiluminescence[15,16] may lead to very effective hybridization sensors.

Another possible approach involves association of two exogenous redox centers to the complementary strands of DNA either through intercalation or covalent attachment via the terminal phosphate[18] or via a modified sugar.[19] Formation of the double helix leads to strong coupling between the redox centers and consequently to high rates of electron transfer between the two redox centers.[20,21] These high rates are believed to result from unique properties of the π stack that

† Present address: Department of Chemistry, Otterbein College, Westerville, OH 43081.

[⊗] Abstract published in *Advance ACS Abstracts*, August 15, 1995.

(1) Jenkins, Y.; Barton, J. K. *J. Am. Chem. Soc.* **1992**, *114*, 8736−8738.
(2) Ried, T.; Baldini, A.; Rand, T. C.; Ward, D. C. *Proc. Natl. Acad. Sci. U.S.A.* **1992**, *89*, 1388−1392.
(3) Du, Z.; Hood, L.; Wilson, R. K. *Methods Enzymol.* **1993**, *218*, 104−121.
(4) Tizard, R.; Cate, R. L.; Ramachandran, K. L.; Wysk, M.; Voyta, J. C.; Murphy, O. J.; Bronstein, I. *Proc. Natl. Acad. Sci. U.S.A.* **1990**, *87*, 4514−4518.
(5) Kaiser, R.; Hunkapiller, T.; Heiner, C.; Hood, L. *Methods Enzymol.* **1993**, *218*.
(6) Maher, L. J., III. *Biochemistry* **1992**, *31*, 7587−7594.
(7) Strobel, S. A.; Dervan, P. B. *Science* **1990**, *249*, 73−75.
(8) Fodor, S. P. A.; Rava, R. P.; Huang, X. C.; Pease, A. C.; Holmes, C. P.; Adams, C. L. *Nature* **1993**, *364*, 555−556.
(9) Noble, D. *Anal. Chem.* **1995**, *67*, 201A-204A.
(10) Bains, W. *Chem. Br.* **1995**, 122−125.
(11) Lishanski, A.; Ostrander, E. A.; Rine, J. *Proc. Natl. Acad. Sci. U.S.A.* **1994**, *91*, 2674−2678.
(12) Youil, R.; Kemper, B. W.; Cotton, R. G. H. *Proc. Natl. Acad. Sci. U.S.A.* **1995**, *92*, 87−91.
(13) Saleeba, J. A.; Cotton, R. G. H. *Methods Enzymol.* **1993**, *217*, 286−295.
(14) Millan, K. M.; Mikkelsen, S. R. *Anal. Chem.* **1993**, *65*, 2317−2323.
(15) Xu, X.-H.; Bard, A. J. *J. Am. Chem. Soc.* **1995**, *117*, 2627−2631.
(16) Xu, X.-H.; Yang, H. C.; Mallouk, T. E.; Bard, A. J. *J. Am. Chem. Soc.* **1994**, *116*, 8386−8387.
(17) Millan, K. M.; Saraullo, A.; Mikkelsen, S. R. *Anal. Chem.* **1994**, *66*, 2943−2948.
(18) Murphy, C. J.; Arkin, M. R.; Jenkins, Y.; Ghatlia, N. D.; Bossmann, S. H.; Turro, N. J.; Barton, J. K. *Science* **1993**, *262*, 1025−1029.
(19) Meade, T. J.; Kayyem, J. F. *Angew. Chem., Int Ed. Engl.* **1995**, *34*, 352−354.
(20) Purugganan, M. D.; Kumar, C. V.; Turro, N. J.; Barton, J. K. *Science* **1988**, *241*, 1645−1649.
(21) Risser, S. M.; Beratan, D. N.; Meade, T. J. *J. Am. Chem. Soc.* **1993**, *115*, 2508−2510.

0002-7863/95/1517-8933$09.00/0

would be present only in the double helix and not in single strands.[22] Using this approach to detect hybridization has not been described explicitly in the literature; however, the experiments do rely on special features of the double helix and therefore may present a means for detecting duplex DNA in the presence of excess single-stranded DNA.

Reported here is a new approach to both detecting hybridization and differentiating single-base mismatches in a single experiment. In this approach, the rate constant for one-electron oxidation of guanine bases in DNA by transition-metal mediators is measured using catalytic cyclic voltammetry. Because the cationic transition-metal mediators interact in the minor groove of DNA,[23-25] intimate contact between the mediator and guanine is precluded by the unique structure of the double helix. This protection of the guanine residue necessitates that the electron tunnels through solvent over some finite distance, which attenuates the rate of electron transfer. The solvent accessibility varies with the nature of the base opposite guanine, which changes the tunneling distance. The electron-transfer rate constant can therefore be used to identify the paired (or mismatched) base. In addition to applications in sequencing or detection of hybridization, this approach may also provide a means for quantitating the solvent accessibility of nucleobases in complex nucleic acid polymers.

Experimental Section

Metal complex mediators of Ru(II) and Fe(II) were prepared as described in the literature.[26] $M(bpy)_3^{3+}$ complexes (M = Fe, Ru) were generated chemically by oxidation of the corresponding $M(bpy)_3^{2+}$ with PbO_2 in 6 M H_2SO_4.[27]

Cyclic Voltammetry. Cyclic voltammograms were collected using a PAR 273A potentiostat/galvanostat with a single-compartment voltammetric cell[28] equipped with an indium tin oxide (ITO) working electrode (area = 0.32 cm^2), a Pt-wire counter electrode, and an Ag/AgCl reference electrode. In a typical experiment, a sample containing 50 μM metal complex and 3.0 mM calf thymus DNA (per nucleotide phosphate) dissolved in buffered aqueous solutions containing 700 mM NaCl and 50 mM Na-phosphate buffer (pH = 6.8, $[Na^+]$ = 780 mM) was scanned at 25 mV/s from 0.0 V to at least 200 mV beyond the redox couple of the metal complex. Scans of polynucleotides in the absence of metal complex showed no appreciable oxidative current to 1.3 V vs Ag/AgCl. Typical DNA backgrounds are given in ref 28. A freshly-cleaned ITO electrode was used for each experiment, and a background scan of buffer alone was collected for each electrode and subtracted from subsequent scans. Calf thymus DNA (sodium salt, type I, Sigma) was slowly dissolved in aqueous buffer to obtain a homogenous solution and stored at 4 °C. Concentrations of DNA (per nucleotide phosphate) were determined spectrophotometrically (ϵ_{260} = 6600 M^{-1} cm^{-1}). Second-order guanine oxidation rate constants were determined by fitting of cyclic voltammetric data to a two-step mechanism using the DigiSim software package.[29] The same rate constant was obtained over a range of scan rates (25 mV/s to 1 V/s). All parameters other than the oxidation rate (e.g., diffusion coefficients, heterogeneous electron-transfer rates, $E_{1/2}$'s) were determined from a voltammogram of the metal complex alone on the same electrode. The diffusion coefficient of DNA was 2.0 × 10^{-7} cm^2/s for calf thymus DNA.[30,31] For $Fe(bpy)_3^{2+}$, the oxidized metal complex reacted by some pathway independent of DNA oxidation to form another species, which was apparent at some scan rates. In this case, an additional step was added to the mechanism, and the rate for that process was determined from a voltammogram of the metal complex without DNA. If the rate of DNA oxidation was exceptionally high (e.g., $Ru(bpy)_3^{2+}$), a second oxidation step was added to the mechanism to account for overoxidation of guanine products, as observed in related systems.[32]

Square-wave voltammograms were collected using the same apparatus and conditions described for cyclic voltammetry. The pulse height was 25 mV, the frequency was 20 Hz, and the scan increment was 2.0 mV. Pseudo-first-order oxidation rate constants were determined by fitting the forward and reverse currents to an EC′ mechanism using the COOL software package.[33] Plots of pseudo-first-order rate constants vs concentration of guanine nucleotide were linear, giving the appropriate second-order rate constants.

Stopped-flow data were collected using an OLIS RSM-1000 rapid scanning monochromater. The calf thymus DNA was kept in large excess to ensure psuedo first-order conditions. The reaction was monitored spectrophotometrically from 300–600 nm for times ranging from 1.0 s (1000 scans/s) to 30 s (20 scans/s) depending on the rate of oxidation. Second-order oxidation rate constants were determined by global analysis[34] of all the data using the SPECFIT software obtained from Spectrum Software Associates, Chapel Hill, NC.

Synthetic oligonucleotides (15-mer sequences given inTable 2) were synthesized locally (UNC Department of Pathology) and purified using HPLC [PerSeptive Self-Pack POROS 20 R2 column, triethylamine acetate buffer (pH = 5.8) + 5% CH_3CN gradient with 100% CH_3CN], lyophylized, converted to the Na^+ salt, and dissolved in 700 mM NaCl/50 mM sodium phosphate buffer. Concentrations of oligonucleotides were determined spectrophotometrically.[35] A typical sample contained 25 μM $Ru(bpy)_3^{2+}$ and 100 μM oligonucleotide (per oligonucleotide). Scans of the single-stranded oligonucleotides that did not contain guanine and $Ru(bpy)_3^{2+}$ showed negligible currents. Hybridization of the oligonucleotides was accomplished by combining the guanine-containing oligonucleotide with a slight excess of its complement, heating to 90 °C for 5 min, then slow cooling over 2 h to 25 °C. The calculated T_m's[36] of all double-stranded oligonucleotides (including mismatches) were above 35 °C, indicating stable duplex formation under

Table 1. Rate Constants for Oxidation of Guanine in Calf Thymus DNA by Metal Complexes

metal complex	$E_{1/2}$ (V)	D (cm^2/s)	k (M^{-1} s^{-1})[a]
$Ru(bpy)_3^{3+}$	1.06	6.0 × 10^{-6}	9.0 × 10^3 [b]
			24 × 10^3 [d]
			8.2 × 10^3 [c]
$Ru(5,6\text{-}Me_2\text{-}phen)_3^{3+}$	1.01	7.3 × 10^{-6}	3.2 × 10^3 [b]
			3.5 × 10^3 [c]
$Fe(5\text{-}Cl\text{-}phen)_3^{3+}$	0.99	5.0 × 10^{-6}	2.6 × 10^3 [b]
			2.5 × 10^3 [c]
$Ru(4,4'\text{-}Me_2\text{-}bpy)_3^{3+}$	0.88	4.3 × 10^{-6}	230[b]
			280[c]
$Fe(bpy)_3^{3+}$	0.85	6.0 × 10^{-6}	210[c]
			420[d]

[a] DNA concentrations used to determine rate constants were based on the moles of guanine nucleotides. Potentials are versus Ag/AgCl. [b] Measured by fitting catalytic cyclic voltammograms of the 2+ ion in the presence of DNA using DigiSim. [c] Measured by fitting catalytic square-wave voltammograms with COOL to determine k_{obsd}. Rate constants were obtained from linear plots of k_{obsd} vs [DNA]. [d] Determined by stopped-flow spectrophotometry experiments on the 3+ metal complex mixed with DNA. Rate constants were obtained from fitting of the complete time-dependent spectra using SPECFIT. Ligand abbreviations: 5,6-Me_2-phen = 5,6-dimethyl-1,10-phenanthroline; 5-Cl-phen = 5-chlorophenanthroline; 4,4′-Me_2-bpy = 4,4′-dimethyl-2,2′-bipyridine.

(22) Stemp, E. D. A.; Arkin, M. R.; Barton, J. K. *J. Am. Chem. Soc.* **1995**, *117*, 2375–2376.
(23) Pyle, A. M.; Rehmann, J. P.; Meshoyrer, R.; Kumar, C. V.; Turro, N. J.; Barton, J. K. *J. Am. Chem. Soc.* **1989**, *111*, 3051.
(24) Cheng, C.-C.; Goll, J. G.; Neyhart, G. A.; Welch, T. W.; Singh, P.; Thorp, H. H. *J. Am. Chem. Soc.* **1995**, *117*, 2970–2980.
(25) Satyanarayana, S.; Dabrowiak, J. C.; Chaires, J. B. *Biochemistry* **1992**, *31*, 9319.
(26) Kalyanasundaram, K. *Coord. Chem. Rev.* **1982**, *46*, 159.
(27) DeSimone, R. E.; Drago, R. S. *J. Am. Chem. Soc.* **1970**, *92*, 2343.
(28) Johnston, D. H.; Cheng, C.-C.; Campbell, K. J.; Thorp, H. H. *Inorg. Chem.* **1994**, *33*, 6388–6390.
(29) Rudolph, M.; Reddy, D. P.; Feldberg, S. W. *Anal. Chem.* **1994**, *66*, 589A.
(30) Welch, T. W.; Corbett, A. H.; Thorp, H. H. *J. Phys. Chem.* **1995**, *99*, 11757–11763.
(31) Tracy, M. A.; Pecora, R. *Ann. Rev. Phys. Chem.* **1992**, *43*, 525.
(32) Neyhart, G. A.; Cheng, C.-C.; Thorp, H. H. *J. Am. Chem. Soc.* **1995**, *117*, 1463–1471.
(33) Osteryoung, J. *Acc. Chem. Res.* **1993**, *26*, 77.
(34) Maeder, M.; Zuberbühler, A. D. *Anal. Chem.* **1990**, *62*, 2220.
(35) Fasman, G. D. *CRC Handbook of Biochemistry and Molecular Biology*; CRC Press: Boca Raton, FL, 1975; Vol. 1.

Table 2. Rate Constants for Oxidation of Guanine in DNA Oligomers by $Ru(bpy)_3^{2+}$

k (M^{-1} s^{-1})[a]	oligomer sequence	Δr_{Ru-G} (Å)[b]
1.2×10^3	(5′-AAATATAGTATAAAA)•(3′-TTTATATCATATTTT) (GC pair)	1.7
5.1×10^3	(5′-AAATATAGTATAAAA)•(3′-TTTATATCTTATTTT) (GC pair adjacent to a TT mismatch)	1.2
5.1×10^3	(5′-AAATATAGTATAAAA)•(3′-TTTATATTATATTTT) (GT mismatch)	1.2
1.0×10^4 [c]	(5′-AAATATAGTATAAAA)•(3′-TTTATATGATATTTT) (GG mismatch)	1.0
1.9×10^4	(5′-AAATATAGTATAAAA)•(3′-TTTATATAATATTTT) (GA mismatch)	0.7
1.8×10^5	(5′-AAATATAGTATAAAA) (single strand)	0

[a] DNA concentrations used to determine rate constants were based on the moles of guanine nucleotides. Diffusion coefficients for all oligomers were fixed at 1.0×10^{-5} cm^2/s. [b] Estimated distance of tunneling through solvent. Distances calculated according to $k/k_{ss} = \exp[-\beta\Delta r]$, where $\beta(H_2O) = 3$ $Å^{-1}$ and $k_{ss} = 1.8 \times 10^5$ M^{-1} s^{-1}. [c] Since the rate constants are relative to guanine concentrations, the observed rate for the GG mismatch has been normalized relative to the other oligomers containing a single guanine.

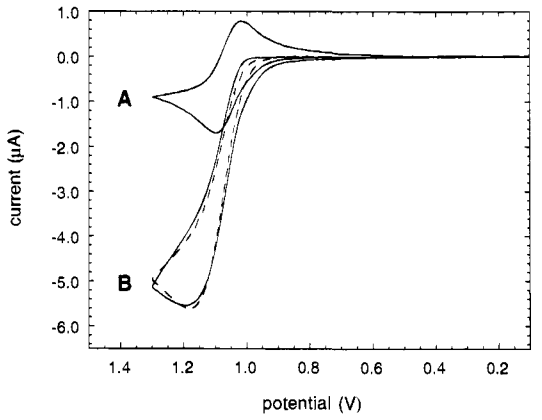

Figure 1. Cyclic voltammograms of $Ru(bpy)_3^{2+}$ and calf thymus DNA. (A) Scan of 50 μM $Ru(bpy)_3^{2+}$ at 25 mV/s in 700 mM NaCl/50 mM sodium phosphate buffer. (B) Voltammogram of 50 μM $Ru(bpy)_3^{2+}$ and 3.0 mM (nucleotide) calf thymus DNA (solid line). (B) Simulated cyclic voltammogram using DigiSim with $k_{ox} = 9.0 \times 10^3$ M^{-1} s^{-1} (dashed line).

the conditions used ($[Na^+] = 780$ mM). Rate constants are given in terms of concentration of guanine.

Results and Discussion

Guanine–Metal Electron Transfer. We have reported previously that metal complexes based on $ReO_2(py\text{-}x)_4^{2+}$ and $M(bpy)_3^{3+}$ oxidize DNA by outer-sphere electron transfer in guanine-containing polymers when the potential of the metal complex is >0.9 V (all potentials vs Ag/AgCl, py-x = substituted pyridine, bpy = 2,2′-bipyridine).[28,37] High-resolution electrophoresis experiments verify that this oxidation occurs specifically at guanine residues. We have observed catalytic current in cyclic voltammograms of the metal complexes in the presence of DNA,[28] indicating that multiple turnovers of oxidation of DNA by the oxidized form of the metal complex are observed during a single voltammetric sweep. As discussed below, analysis of this catalytic enhancement allows for determination of the rate of guanine oxidation by the metal complex.

Shown in Figure 1 are the cyclic voltammograms of $Ru(bpy)_3^{2+}$ with and without calf thymus DNA, showing the catalytic enhancement. The voltammetry of any DNA-bound redox couple must be analyzed in terms of a square scheme that relates the bound and unbound forms[38–40] because the diffusion coefficient of DNA is much lower (2.0×10^{-7} cm^2/s) than that of the metal complex (6.0×10^{-6} cm^2/s).[30,31] This phenomenon generally leads to dramatically decreased currents for the bound form;[39] however, at sufficiently high ionic strength ($[Na^+] = 0.78$ M), binding of the metal complex is too weak to influence the current response. In this case, the current can be analyzed in terms of a simple EC′ mechanism:

$$Ru(bpy)_3^{2+} \rightarrow Ru(bpy)_3^{3+} \quad (E) \qquad (1)$$

$$Ru(bpy)_3^{3+} + DNA \rightarrow Ru(bpy)_3^{2+} + DNA_{ox} \quad (C') \qquad (2)$$

Cyclic voltammograms were analyzed by fitting the complete current–potential curves (background-subtracted) using the DigiSim analysis package.[29] The input parameters were the $E_{1/2}$ for the metal complex and the diffusion coefficients for the metal complex and the DNA, all of which are well determined in separate experiments. Therefore, the sole parameter obtained from the fit was the second-order rate constant for eq 2, $k = 9.0 \times 10^3$ M^{-1} s^{-1}. The same rate constant was determined over a wide range of scan rates (25 mV/s to 1 V/s), and the high quality of the fit is apparent in Figure 1.

The rate constant for oxidation of DNA by $Ru(bpy)_3^{3+}$ was confirmed in two separate experiments. First, square-wave voltammograms under conditions of excess DNA were used to obtain a pseudo-first-order k_{obsd} for eq 2 by fitting with the COOL algorithm.[33] The COOL algorithm uses a fitting approach that is significantly different from DigiSim; nevertheless, plots of k_{obsd} against [DNA] were linear and gave a second-order rate constant $k = 8.2 \times 10^3$ M^{-1} s^{-1}, which was in agreement with that obtained from fitting cyclic voltammograms with DigiSim. Signal-to-noise in the square-wave experiments was lower than for cyclic voltammetry because concentrations ensuring a psuedo-first-order excess of DNA were required, limiting the quantities of metal complex that could be used. Sample data for this method using $Fe(bpy)_3^{2+}$ are shown in Figure 2.

Second, authentic samples of $Ru(bpy)_3^{3+}$ were prepared and reacted with DNA directly in a rapid-scanning stopped flow. Global analysis of the time-dependent spectra between 350 and 600 nm[34] showed that $Ru(bpy)_3^{3+}$ was converted cleanly to $Ru(bpy)_3^{2+}$ with no intermediates and a rate constant of 24×10^3 M^{-1} s^{-1} (Figure 3). The spectra calculated from the global analysis agree well with the known spectra of $Ru(bpy)_3^{2+}$ and

(36) Maniatis, T.; Fritsch, E. F.; Sambrook, J. *Molecular Cloning: A Laboratory Manual*, 2nd ed.; Cold Spring Harbor Press: Plainview, NY, 1989.
(37) Federova, O. S.; Podust, L. M. *J. Inorg. Biochem.* **1988**, *34*, 149–155.
(38) Carter, M. T.; Bard, A. J. *Bioconjugate Chem.* **1990**, *1*, 257.
(39) Carter, M. T.; Rodriguez, M.; Bard, A. J. *J. Am. Chem. Soc.* **1989**, *111*, 8901.
(40) Carter, M. J.; Bard, A. J. *J. Am. Chem. Soc.* **1987**, *109*, 7528–7530.

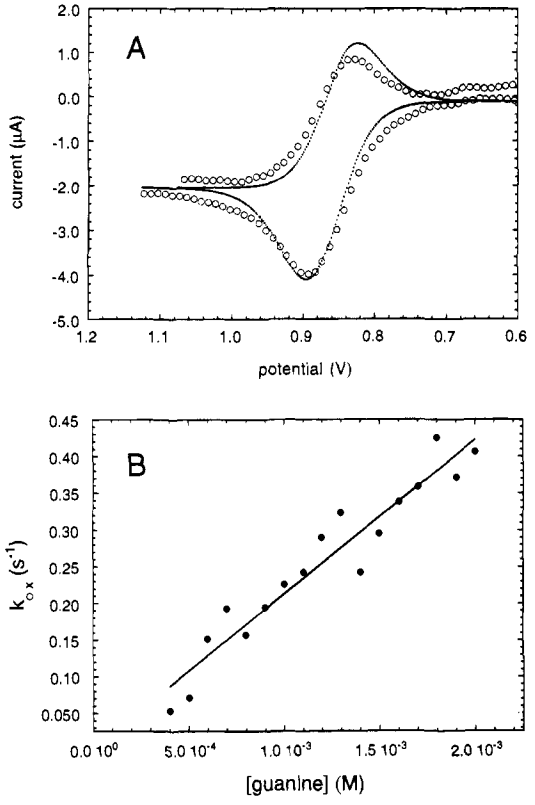

Figure 2. (A) Forward and reverse current from the square-wave voltammogram of $Fe(bpy)_3^{2+}$ and DNA (circles) with COOL fit for EC′ mechanism superimposed (solid line). Conditions: 50 μM $Fe(bpy)_3^{2+}$, 4.7 mM calf thymus DNA, electrochemical parameters given in the Experimental Section. (B) Dependence of k_{obsd} determined by COOL on concentration of DNA, giving $k = 210\ M^{-1}\ s^{-1}$.

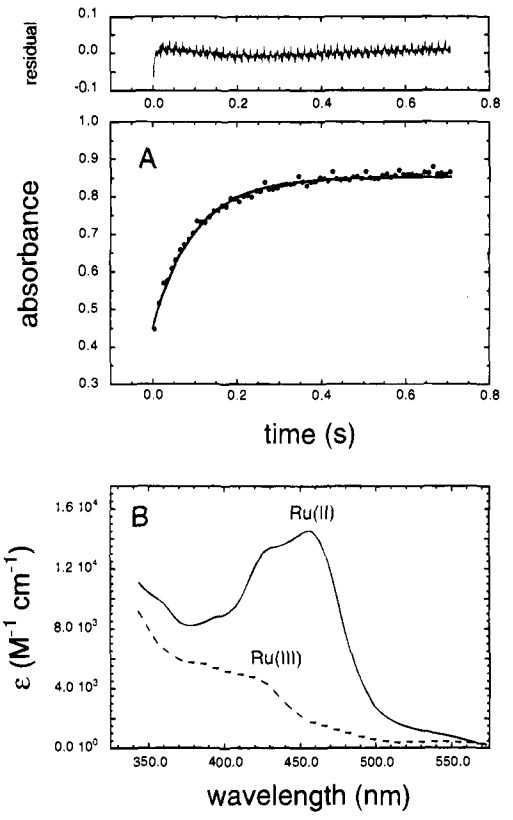

Figure 3. (A) Absorbance at 456 nm versus time for oxidation of calf thymus DNA by $Ru(bpy)_3^{3+}$. Solid line shows calculated time dependence from global analysis, $k = 24 \times 10^3\ M^{-1}\ s^{-1}$. (B) Calculated spectra of $Ru(bpy)_3^{2+}$ and $Ru(bpy)_3^{3+}$ determined in the SPECFIT global analysis.

$Ru(bpy)_3^{3+}$.[26] Thus, the rate constant for DNA oxidation by $Ru(bpy)_3^{3+}$ was firmly established by two independent electrochemical measurements with dramatically different fitting protocols and by a nonelectrochemical stopped-flow technique with fitting of the complete visible spectra.

Driving-Force Dependence. Understanding the dependence of electron-transfer rates on distance and driving force is an area of active experimentation and high theoretical sophistication.[21,41-46] If the driving force for electron transfer is significantly less than the reorganizational energy (λ), a plot of $RT \ln k$ versus driving force (when corrected for work terms associated with approach of the reactants,[47] see figure legend) should yield a straight line with a slope of $^1/_2$.[48] The rate constants for oxidation of DNA by a number of $M(bpy)_3^{3+}$ derivatives with different redox potentials are shown in Table 2. A Marcus plot of these rate constants and driving forces is shown in Figure 4, where the slope and linearity are in excellent agreement with the theoretical prediction.

Having demonstrated that Marcus theory describes the driving-force dependence of the electron-transfer rate, we can

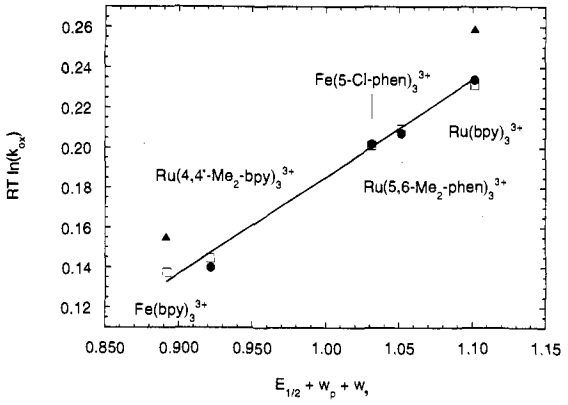

Figure 4. Driving force dependence of the rate constant (Table 1) for electron transfer from guanine in calf thymus DNA to the metal complex. The best fit gave a slope of 0.49. The x axis was corrected for the work involved in approach and separation of the reactants and products, which was calculated from polyelectrolyte theory.[47] Oxidation rates were determined by (circles) cyclic voltammtery with fitting of digitally simulated scans as in Figure 1, (squares) square-wave voltammetry with fitting using the COOL algorithm, and (triangles) stopped-flow spectrophotometry with global fitting.

now analyze the absolute rate constants in terms of the general equation:[44-46]

$$k = \nu \exp[-\beta(r - r_0)] \exp[-(\Delta G + \lambda)^2/4\lambda RT] \quad (3)$$

where ν is the rate constant in the diffusion-controlled limit ($10^{11}\ M^{-1}\ s^{-1}$), r is the distance between reactant and product

(41) Beratan, D. N.; Onuchic, J. N.; Winkler, J. R.; Gray, H. B. *Science* **1992**, *258*, 1740-1741.
(42) Bowler, B. E.; Raphael, A. L.; Gray, H. B. *Prog. Inorg. Chem.* **1990**, *38*, 259-322.
(43) McCleskey, T. M.; Winkler, J. R.; Gray, H. B. *J. Am. Chem. Soc.* **1992**, *114*, 6935-6937.
(44) Wuttke, D. S.; Gray, H. B. *Curr. Opin. Struct. Biol.* **1993**, *3*, 555-563.
(45) Moser, C. C.; Keske, J. M.; Warncke, K.; Farid, R. S.; Dutton, P. L. *Nature* **1992**, *355*, 796-802.
(46) Wuttke, D. S.; Bjerrum, M. J.; Winkler, J. R.; Gray, H. B. *Science* **1992**, *256*, 1007-1009.
(47) Kalsbeck, W. A.; Thorp, H. H. *J. Am. Chem. Soc.* **1993**, *115*, 7146-7151.
(48) Bock, C. R.; Connor, J. A.; Gutierrez, A. R.; Meyer, T. J.; Whitten, D. G.; Sullivan, B. P.; Nagle, J. K. *J. Am. Chem. Soc.* **1979**, *101*, 4815.

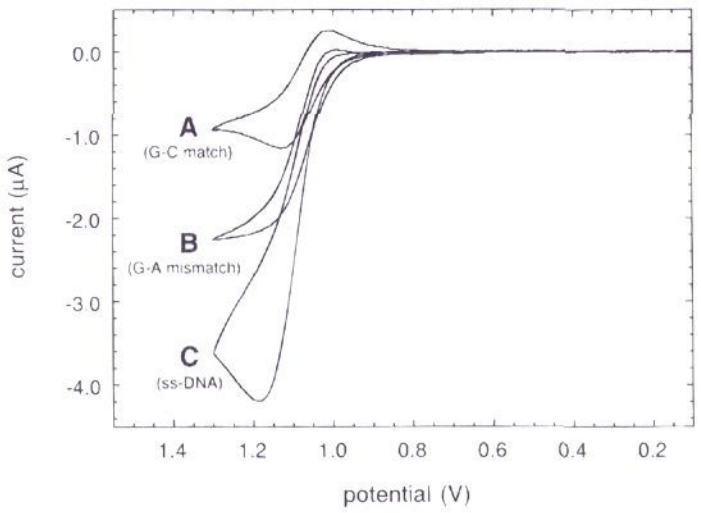

Figure 5. Cyclic voltammograms of $Ru(bpy)_3^{2+}$ with double-stranded and single-stranded oligonucleotides (scan rate = 25 mV/s). (A) 25 μM $Ru(bpy)_3^{2+}$ + 100 μM (in guanine nucleotides) double-stranded fully hybridized DNA (5′-AAATATAGTATAAAA)·(3′-TTTATATCATATTTT). (B) $Ru(bpy)_3^{2+}$ with a duplex containing a GA mismatch (5′-AAATATAGTATAAAA)·(3′-TTTATATAATATTTT). (C) $Ru(bpy)_3^{2+}$ + a single strand containing one guanine nucleotide (5′-AAATATAGTATAAAA).

in the activated complex, r_o is the distance of closest approach of reactant and product, and β describes the influence of the intervening medium. Incorporation of the guanine donor into the interior of the double helix imposes a finite distance across which the electron must tunnel to the bound metal complex, i.e. $r \neq r_o$. However, if guanosine 5′-monophosphate (GMP) is used as the electron donor, direct collision of guanine with the metal complex is possible ($r = r_o$). For $Fe(bpy)_3^{3+}$ and GMP, the rate constant measured by stopped-flow is 2.6×10^3 M^{-1} s^{-1}. The quantity $\exp[-\beta(r - r_o)]$ is therefore estimated as the ratio k_{DNA}/k_{GMP}. Known values of λ for related reactions are in the range 1−1.5 eV,[44,49,50] which give a ΔG for the guanine$^{+/0}$ couple of 1.1 ± 0.1 V using eq 3. Implicit in this estimate is the assumption that λ and ΔG are the same for guanine in aqueous solution and in the double helix, which may alter the calculated ΔG somewhat through outer-sphere solvent effects;[50] however, the estimate is in reasonable agreement with related estimates from kinetic data from pulse radiolysis.[51]

Distance Dependence. Shown in Figure 5 are the cyclic voltammograms of $Ru(bpy)_3^{2+}$ in the presence of 5′-AAATATAGTATAAAA as a single strand (Figure 5C) and hybridized to its complementary strand (Figure 5A). As with GMP, $r = r_o$ for the single strand, and the rate constant of 1.8×10^5 M^{-1} s^{-1} gives $\Delta G(\text{guanine}^{+/0}) = 1.1$ V and $\lambda = 1.3$ eV, which are in agreement with the values from GMP oxidation. While there is a dramatic enhancement for the single strand, a much smaller enhancement is observed for the fully hybridized duplex, resulting in a 4-fold reduction in current upon hybridization.[52] Metal complexes such as $Ru(bpy)_3^{2+}$ are known to interact with DNA in the minor groove,[23−25,53] so the 150-fold slower rate constant (1.2×10^3 M^{-1} s^{-1}) for oxidation of the duplex must result from the distance between the guanine residue and the surface-bound complex. One possible collision geometry is shown in Figure 6 where guanine and the metal complex cannot come into intimate contact and the electron must therefore tunnel through the solvent that separates the guanine residue and the metal complex. Tunneling through water is much less efficient than through nonpolar media, and the value of β for H_2O is estimated to be about 3 $Å^{-1}$ compared to 1 $Å^{-1}$ for proteins.[41,44,45] The tunneling distance can therefore be estimated according to:

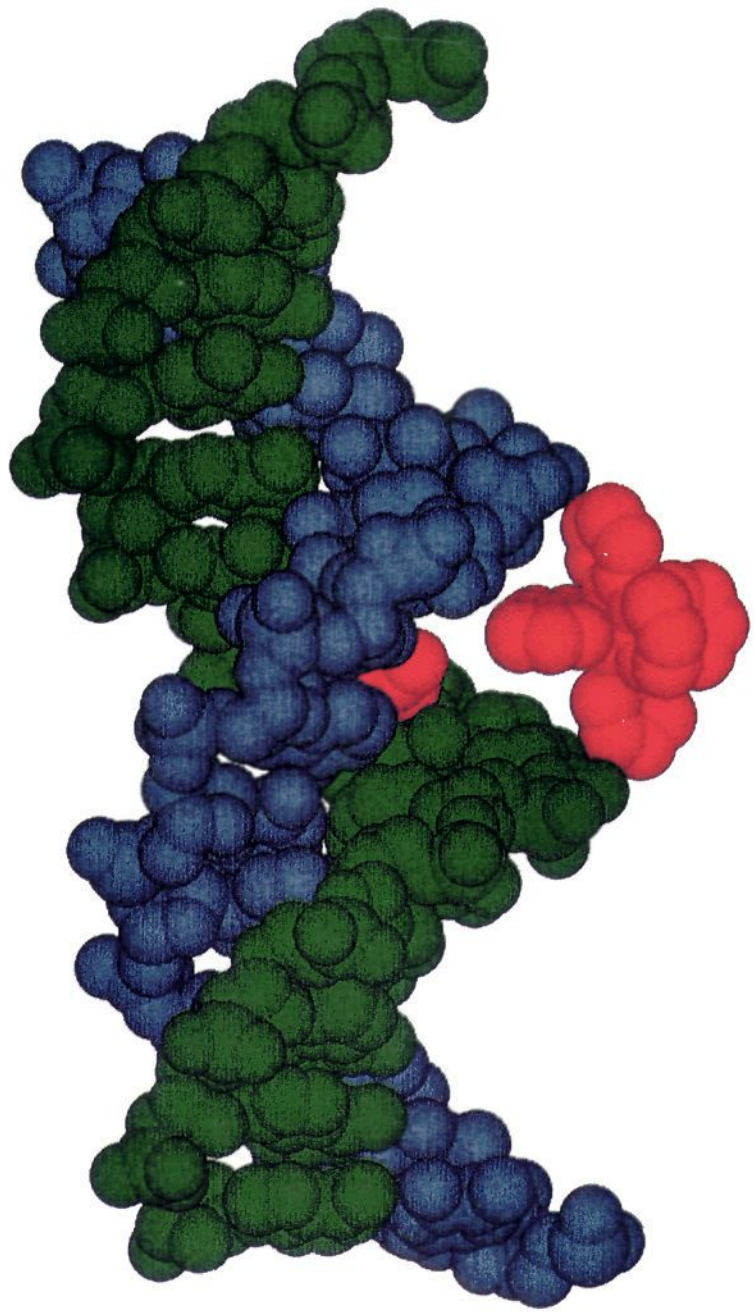

Figure 6. Computer-generated space-filling diagram illustrating a possible collision geometry for $Ru(bpy)_3^{2+}$ (red) in the minor groove of DNA (green and blue). The guanine residue is shown in red, and the white area in between guanine and $Ru(bpy)_3^{2+}$ illustrates that electron transfer within intimate contact cannot occur with double-helical DNA.

$$k/k_{ss} = \exp(-\beta\Delta r) \quad (4)$$

where Δr is the change in distance in the duplex compared to the single strand and k_{ss} is the rate constant for oxidation of guanine in the single strand where $r = r_o$. From this analysis, Δr for the fully hybridized duplex is 1.7 Å. We have neglected effects arising from nonproductive collisions of the metal complex with the oligomer in regions where no guanine is present. These considerations would introduce an orientation factor into eq 3; however, since the duplex and single strand are the same length, the number of possible nonproductive collisions is probably similar for both.

The large value of β for water suggests that significant changes in the electron-transfer rate constants will be effected by very small changes in the tunneling distance, which could

(49) Karas, J. L.; Lieber, C. M.; Gray, H. B. *J. Am. Chem. Soc.* **1988**, *110*, 599.

(50) Marcus, R. A.; Sutin, N. *Biochim. Biophys. Acta* **1985**, *811*, 265.

(51) Candeias, L. P.; Steenken, S. *J. Am. Chem. Soc.* **1993**, *115*, 2437−2440. Steenken, S. *Chem. Rev.* **1989**, *89*, 503−520.

(52) The rate constant is somewhat slower for the 15-mer duplex compared to calf thymus DNA. In calf thymus DNA, numerous sequences are present, so the measured rate constant represents the reactivity of an ensemble of sequences, many of which may be more efficiently oxidized than that selected for the oligomer studies. In particular, guanines adjacent to another guanine are considerably easier to oxidize (see: Saito, I.; Takayama, M.; Sugiyama, H.; Nakatani, K.; Tsuchida, A.; Yamamoto, M. *J. Am. Chem. Soc.* **1995**, *117*, 6406−6407) and may well react at much faster rates than the particular sequence discussed here.

(53) Barton, J. K.; Danishefsky, A. T.; Goldberg, J. M. *J. Am. Chem. Soc.* **1984**, *106*, 2172−2176.

in turn reflect small perturbations in the DNA structure. Also shown in Figure 5 is the voltammogram of $Ru(bpy)_3^{2+}$ in the presence of the same duplex where the GC base pair has been replaced by a GA mismatch (GA). Incorporation of the GA mismatch results in a 2-fold enhancement in the raw current compared to the authentic duplex, which translates to a 16-fold change in rate constant ($k_{GA} = 1.9 \times 10^4\ M^{-1}\ s^{-1}$). The rate data for the single strand, fully hybridized duplex, and all three GX mismatches are set out in Table 2. *All four GX (X = A, T, G, C) oligomers exhibit rate constants that are different and readily distinguished using cyclic voltammetry.* Thus, the guanine−metal tunneling is capable not only of detecting a single-base mismatch but also of determining the nature of the other base within the mismatch.

In addition to detecting mismatches at guanine, an oligomer was also designed with a TT mismatch on the 3′ side of a GC pair to determine if mismatches *adjacent* to guanine could also be detected. In fact, the rate constant for the GC pair adjacent to a TT mismatch is the same as for the duplex where the oxidized guanine is mispaired in a GT mismatch, so an adjacent mismatch does give a rate constant that is detectably different from that of the authentic duplex. The rate constant for this oligomer is also given in Table 2.

Also shown in Table 2 are the tunneling distances Δr relative to the single strand calculated using $\beta = 3\ Å^{-1}$. As expected, the guanine residue in G-purine mismatches is more accessible to the metal complex than in the GT mismatch, where the two bases are still joined by two hydrogen bonds in a wobble pair.[54] Nonetheless, the GT mismatch still causes a 4-fold change in rate constant, which is readily detectable.

Conclusions

These results present a new means for sensitively detecting the solvent accessibility of individual functionalities in complex nucleic acid polymers. The large value of $\beta(H_2O)$ allows for the discrimination of very small perturbations in DNA structure via the guanine−metal electron-transfer rate constant. Recent efforts on inner-sphere guanine oxidation have shown that the extent of oxidation is related to solvent accessibility.[55] Using the approach described here, the solvent accessibility of numerous functionalities can be determined simply by matching the redox potential of the mediator to the chemical moiety. The A, T, and C bases all exhibit redox chemistry at potentials that are accessible to similar metal complex mediators,[51,56] and related strategies for determining the accessibility of these or derivatized bases can be designed on the basis of the principles described here.

These results may also provide a basis for a new approach to mismatch-sensitive hybridization detection or sequencing. A factor of 2 in rate constant, which would still be readily detectable based on raw current, would give a change in distance compared to that of the authentic duplex of only 0.2 Å. In related strategies where the double helix mediates electron transfer between two exogenous metal complexes,[18,19] electron transfer occurs *parallel* to the helical axis. In the system described here, electron transfer occurs *perpendicular* to the helical axis, which is the direction most likely to be affected by a mismatch. Electrochemical schemes are considerably more economical to implement than laser-based fluorescence detection, and covalent labeling of the DNA is not required to perform the analyses shown in Figure 5.

Acknowledgment. We thank Professor H. B. Gray for helpful discussions concerning the driving force and distance dependences and Dr. C.-C. Cheng for assistance in purifying the oligonucleotides. This work was supported by the David and Lucile Packard Foundation.

JA951311Q

(54) Strobel, S. A.; Cech, T. R. *Science* **1995**, *267*, 675−679.

(55) Chen, X.; Woodson, S. A.; Burrows, C. J.; Rokita, S. E. *Biochemistry* **1993**, *32*, 7610−7616.

(56) Steenken, S.; Telo, J. P.; Novais, H. M.; Candeias, L. P. *J. Am. Chem. Soc.* **1992**, *114*, 4701−4709.